Available online at www.sciencedirect.com
ScienceDirect
ELSEVIER
Nuclear Physics B (Proc. Suppl.) 196 (2009) 341–355
NUCLEAR PHYSICS B PROCEEDINGS SUPPLEMENTS
www.elsevier.com/locate/npbps

Experimental Efforts on Very High-Energy Cosmic Rays and their Interactions — Conference Summary

J.R. Hörandel[a]

[a]Radboud University Nijmegen, Department of Astrophysics, Nijmegen, The Netherlands; j.horandel@astro.ru.nl

Progress reported during the XV International Symposium on Very High-Energy Cosmic-Ray Interactions is summarized. Emphasize is given to experimental work. The actual status, recent results, and their implications on the present understanding of the origin of high-energy cosmic-rays and their interactions are discussed.

1. Introduction

The XV International Symposium on Very High-Energy Cosmic-Ray Interactions (ISVHECRI 2008) took place in Paris from September 1^{st} to 6^{th}, 2008. Main objective of the symposium was to contribute to the understanding of the origin of cosmic rays. The relation between the various topics discussed is shown schematically in Fig. 1. Progress has been reported in the fields of solar particles (Sect. 4), TeV gamma-ray astronomy (Sect. 6), neutrino astronomy (Sect. 7), as well as the direct (Sect. 5) and indirect (Sect. 9) measurements of cosmic rays. To reveal the origin of high-energy cosmic rays combined efforts of TeV gamma-ray astronomy, neutrino astronomy, and cosmic-ray research will become crucial (multi messenger approach). The properties of hadronic interactions are studied in detail at accelerator experiments (Sect. 3). This knowledge contributes to the understanding of high-energy interactions in air showers. Also information deduced from air showers can be used to deduced properties of high-energy interactions in turn (Sect. 8). This is in particular of interest in kinematical and energy regions not covered by accelerator experiments. The (astrophysical) interpretation of air shower data depends critically on our understanding of the properties of high-energy interactions. Thus, accelerator experiments contribute significantly to our understanding of the origin of cosmic rays.

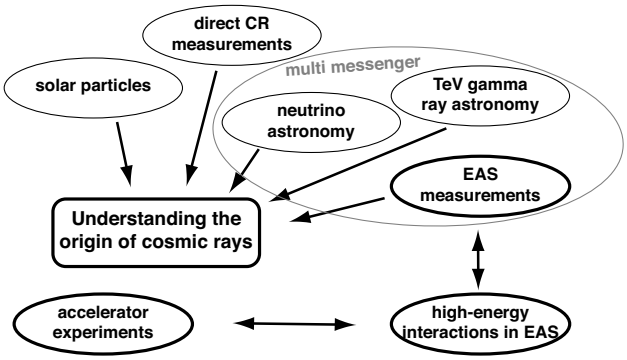

Figure 1. Schematic view of the relations between the topics discussed at the meeting.

The ISVHECRI meeting series has served and should continue to serve in future as bridge between the accelerator and cosmic-ray communities. The relations between this fields should be further strengthened. Thus, improving our knowledge on high-energy interactions on one side, but at the same time also increasing our (astrophysical) understanding of the processes in the Universe.

This article summarizes experimental work presented at the meeting [1]. The actual status, recent results, and their implications on the present un-

[1]Work reported, related to emulsion chambers and theoretical considerations are discussed in separate summaries. Nevertheless, more than 20 h of talks and some 30 posters are expected to be covered by the present article. This is an almost impossible venture, thus, this summary may be biased towards a personal selection of scientific highlights.

0920-5632/$ – see front matter
doi:10.1016/j.nuclphysbps.2009.09.065

derstanding of the origin of very high-energy cosmic rays and their interactions are discussed.

2. High-Energy Cosmic Rays and Extensive Air Showers

The Earth is permanently exposed to a vast flux of high-energy particles from outer space. Most of these particles are ionized atomic nuclei with relativistic energies. They have a threefold origin. Particles with energies below 100 MeV originate from the Sun [1,2]. Cosmic rays in narrower sense are particles with energies from the 100 MeV domain up to energies beyond 10^{20} eV. Up to several 10 GeV the flux of the particles observed at Earth is modulated on different time scales by heliospheric magnetic fields [3,4]. Cosmic rays with energies below 10^{17} to 10^{18} eV are usually considered to be of galactic origin [5–11]. Particles at higher energies can not be magnetically bound to the Galaxy. Hence, they are considered to be of extra-galactic origin [11–15].

When high-energy cosmic rays impinge on the atmosphere of the Earth they initiate cascades of secondary particles — the extensive air showers. Objective of air shower detectors is to derive information about the shower inducing primary particle from the registered secondary particles. Addressing astrophysical questions with air-shower data necessitates the understanding of high-energy interactions in the atmosphere.

For air shower interpretation the understanding of multi-particle production in hadronic interactions with small momentum transfer is essential [16]. Due to the energy dependence of the coupling constant, α_s, soft interactions cannot be calculated within QCD using perturbation theory. Instead, phenomenological approaches have been introduced in different models. These models are the main source of uncertainties in simulation codes to calculate the development of extensive air showers, such as the program CORSIKA [17]. Several codes to describe hadronic interactions at low energies ($E < 200$ GeV; e.g. GHEISHA [18] and FLUKA [19,20]) as well as at high energies (e.g. DPMJET [21], QGSJET [22–24], SIBYLL [25], and EPOS [26,27]) have been embedded in CORSIKA.

3. Accelerator Experiments

3.1. Accelerator data needed for cosmic-ray physics

More information about hadronic interactions is needed from accelerator experiments to fully understand cosmic rays, as discussed in the following.

Air shower measurements

In high-energy interactions most energy is escaping the interaction region in the forward direction, i.e. at large pseudo rapidity values[2], η. For example, the energy flow at the LHC at $E_{cm} = 14$ TeV, corresponding to $E_{lab} = E_{cm}^2/m_p = 10^{17}$ eV, peaks at pseudo rapidity values around 7 to 10. The forward region with values $|\eta| > 4$ is of great importance for air shower experiments.

Of particular interest are the total (inelastic) cross sections, the elasticity/inelasticity of the interactions, as well as the production cross sections of secondary particles and their parameter distributions, like multiplicity, transverse momentum, energy, and pseudorapidity. As projectiles protons and pions are of interest to study the elementary interactions but also beams of heavier nuclei (such as C, N, O, or Fe, being dominant in the primary cosmic-ray composition) are desirable. Targets are preferably air constituents, i.e. nitrogen, oxygen, (and carbon). In particular, at the LHC the study of p-p and p-N interactions is of great importance.

The uncertainties introduced in the proton air cross section by extrapolating from accelerator data to the highest energies is illustrated in Fig. 2 [28]. It is obvious that LHC data will drastically reduce the uncertainties in the regime of the highest-energy cosmic rays.

Direct measurements

Further input from accelerator experiments is also required for the interpretation of data from balloon borne cosmic-ray detectors. The system-

[2]The pseudo rapidity η describes the angle of a particle relative to the beam axis. It is defined as $\eta = -\ln[\tan(\theta/2)]$, where θ is the angle between the particle momentum $\vec{p}$ and the beam axis, or, using the longitudinal component p_L of the particle momentum $\eta = 1/2 \ln[(|\vec{p}| + p_L)/(|\vec{p}| - p_L)]$.

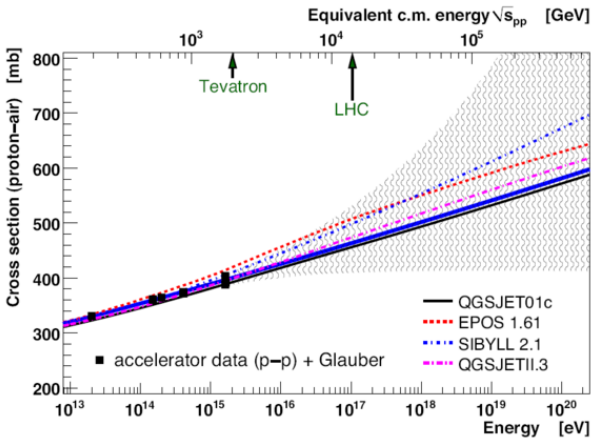

Figure 2. Uncertainties of the extrapolation of the proton-air cross section from accelerator to cosmic-ray energies [28].

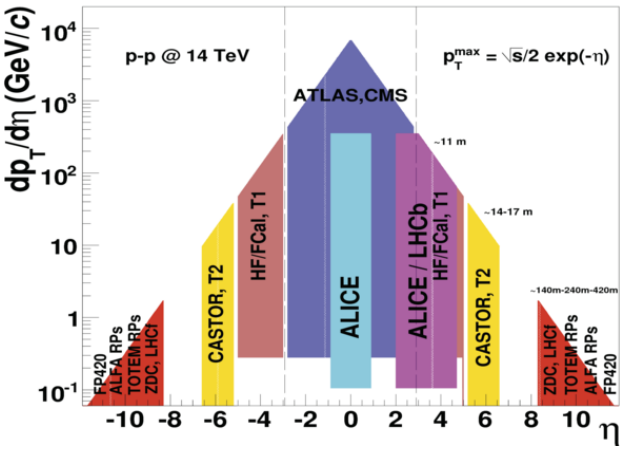

Figure 3. Pseudorapidity ranges covered by various experiments at the LHC [29].

atic uncertainties of measurements of the boron-to-carbon ratio, see Fig. 6, are presently dominated by uncertainties in the production cross section of boron in the residual atmosphere above the detector. Boron is produced through spallation of the relatively abundant elements of the CNO group in the atmosphere [3]. Thus, the production cross sections of boron for protons and CNO nuclei impinging on nitrogen targets are of great interest at energies significantly exceeding 100 GeV/n.

3.2. Present activities

The (re)start of the LHC [30] during 2009 will begin a new era in particle physics. The general purpose detectors ATLAS [31,32] and CMS [33,29] as well as the specialized ALICE [34] and LHCb [35] experiments cover the central collision region with $|\eta| < 4$, see Fig. 3. The most important experiments for air shower physics are experiments exploring the forward region $|\eta| > 4$, such as LHCf [36] and TOTEM [37]. The principle idea is to measure charged particles as close as possible to the beam, sometimes even with detectors inside the beam pipe and to register neutral particles in the forward direction (zero degree detectors).

[3]The detectors float typically below a residual atmosphere of about $3 - 5$ g/cm^2.

LHCf [38,36] comprises two sampling calorimeters (tungsten absorber and scintillator layers), located ±140 m from the ATLAS interaction point and covers pseudo rapidities $|\eta| > 8.5$. Two imaging shower calorimeters are located on the beam axis. One detector uses scintillating fibers and multi-anode PMTs for the read-out, the second calorimeter uses silicon strip sensors. In addition, ATLAS [31] comprises several forward detector systems, namely: LUCID ($5.4 < |\eta| < 6.1$), ALFA, and a zero degree calorimeter (ZDC, $|\eta| > 8.3$).

The TOTEM experiment [37,39] is dedicated to the measurement of the total proton-proton cross section. The detectors are located on both sides of the interaction point close to the CMS experiment and cover the pseudo rapidity range $3.1 \leq |\eta| \leq 6.5$. Two telescopes for inelastically produced charged particles are installed 9 m and 13.5 m from the interaction point, respectively. Two so-called "Roman Pots" are placed 147 m and 220 m from the interaction point, designed to detect leading protons at merely a few mm from the beam center. The CMS experiment [33] comprises also forward detectors: CASTOR ($5.1 < |\eta| < 6.6$) and a ZDC ($|\eta| > 8.3$). New detectors for the extreme forward region are planned for both, ATLAS and CMS at 220 m and 420 m distance from the interaction points.

Also important for air shower physics, are stud-

ies of the properties of hadronic interactions at fixed target experiments [40]. The particle beams for those experiments are extracted from the main accelerator rings, thus, reaching limited energies only. Some of the most important present experiments are BNL-E910, HARP, MIPP, and NA49/NA61.

E910 was a fixed-target proton-nucleus (p-A) experiment performed at the Brookhaven Alternating Gradient Synchrotron (AGS) reaching momenta up to 18 GeV/c [41–43].

HARP is a large solid angle experiment to measure hadron production using proton and pion beams with momenta between 1.5 and 15 GeV/c impinging on many different solid and liquid targets from low to high Z (H-Pb) [44]. The experiment, located at the CERN PS, took data in 2001 and 2002. For the measurement of momenta of produced particles and for the identification of particle types, the experiment includes a large-angle spectrometer, based on a Time Projection Chamber and a system of Resistive Plate Chambers, and a forward spectrometer equipped with a set of large drift chambers, a threshold Čerenkov detector, a time-of-flight wall and an electromagnetic calorimeter. The large angle system uses a solenoidal magnet, while the forward spectrometer is based on a dipole magnet.

The Main Injector Particle Production (MIPP) experiment is operated in the FNAL Meson Line [45–47]. MIPP targets were exposed to 120 GeV/c protons from the Main Injector, and to lower-energy secondary beams of mixed composition. The MIPP detector configuration is fairly similar to the HARP one, with some differences due to the higher momenta probed. Drift chambers are used to track beam particles, and a beam threshold Čerenkov detector is used to tag the beam particle type. Tracks are reconstructed making use of two dipole magnets deflecting secondary particles in opposite directions, plus a TPC, drift chambers, and proportional wire chambers. As for HARP, the TPC, a time-of-flight wall (ToF), and a threshold Čerenkov detector are used for particle identification. In addition, MIPP uses also a Ring Imaging Čerenkov detector (RICH) for high-momentum particles.

The NA49 detector is a wide acceptance spectrometer for the study of hadron production in proton-proton, proton-nucleus, and nucleus-nucleus collisions at the CERN SPS [48]. The main components are 4 large-volume TPCs for tracking and particle identification via dE/dx. Time-of-flight scintillator arrays complement particle identification. Calorimeters for transverse energy determination and triggering, a detector for centrality selection in p+A collisions, and beam definition detectors complete the set-up. The experiment has been upgraded to NA61 (SHINE – SPS Heavy Ion and Neutrino Experiment) [49]. The experimental program till 2013 foresees comprehensive studies of hadron production in proton-proton, proton-nucleus, and nucleus-nucleus interactions, including proton-lead interactions. Also runs with secondary beams (π, K, p) with momenta between 30 and 350 GeV/c are planned, including measurements with a carbon target.

These experiments have offered/will offer large data samples useful for the cosmic-ray community. Data from E910, NA49, and HARP have been published [40]. Results from MIPP and NA61 are expected in the near future.

The experiments BRAHMS [50], PHENIX [51], PHOBOS [52], and STAR [53] at the Relativistic Heavy Ion Collider (RHIC) at Brookhaven National Laboratory study mainly collisions of heavy nuclei [54]. Of interest for the cosmic-ray community are interactions of gold nuclei and deuterons on a gold target at energies $E_{cm} = 200 \cdot A$ GeV. The d-Au interactions [55,56] are very close to p-Au collisions and therefore interesting for air shower physics.

The OPERA [57,58] neutrino oscillation experiment has been designed to prove the appearance of ν_τ in a nearly pure ν_μ beam produced at CERN and detected in the underground Gran Sasso Laboratory, 730 km away from the source. In OPERA, τ leptons resulting from the interaction of ν_τ are produced in target units made of nuclear emulsion films interleaved with lead plates. Data taking has started in Summer 2008.

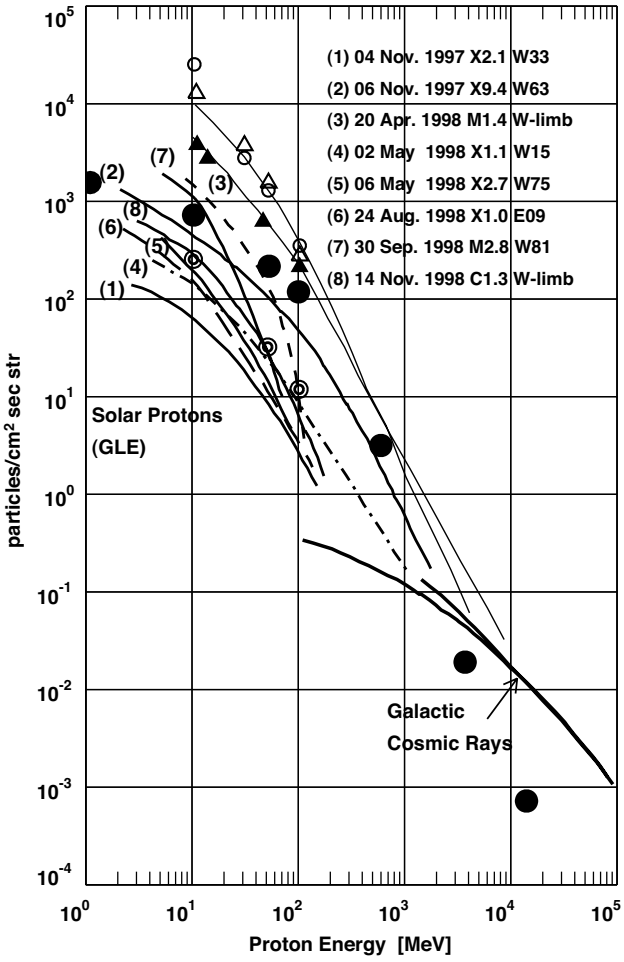

Figure 4. Integral flux of solar protons. Black dots represent the 2001 Easter event, for details see [59,60].

4. Solar Particles

The dynamical motion of magnetic loops at the surface of the Sun is the origin of solar flares [59]. The flares are caused by reconnection of magnetic field lines. This causes the formation of a plasma jet. Plasma particles in the magnetic loop are accelerated by collisions with the high-speed plasma jet from the top of the magnetic loop. The acceleration mechanism is consistent with a shock acceleration picture.

The integral flux of solar protons is shown in Fig. 4 together with the flux of galactic cosmic rays. Depending on the state of the Sun galactic particles start to dominate the overall spectrum at energies exceeding about 100 MeV to 1 GeV. Typically, cosmic particles with energies up to about 100 MeV are assumed to originate from the sun. However, recent measurements indicate that during solar bursts particles can be accelerated to significantly higher energies, exceeding 50 GeV.

A particularly strong solar event occurred on Easter day 2001 (April 15), which has been observed and discussed by several groups [60–66]. The event has been registered with the Karlsruhe Muon Telescope at energies around $10 - 20$ GeV [65]. The GRAND experiment [66] has detected solar energetic particles exceeding 56 GeV. The energy spectrum of the Easter event is presented in Fig. 4 as filled dots. Above 200 MeV the neutron monitor data and the GRAND measurements are described by a single power law with a spectral index $\gamma = -3.75 \pm 0.15$ [59]. This event shows clear evidence that particles with energies exceeding 50 GeV are accelerated at the Sun. It should be noticed that applying the Hillas formula [67] to the Sun yields maximum energies of about 10 TeV.

5. Direct Measurements of Cosmic Rays

With the latest generation of experiments, direct measurements of cosmic rays above the atmosphere now extend to energies around 10^{14} eV with single-element resolution [68]. Spectra for main elements in cosmic rays are summarized in Fig. 5. This compilation covers an enormous range of 7 orders of magnitude in (total particle) energy. To reduce overlap the spectra for individual elements are shifted in vertical direction as indicated. Data are shown from the magnet spectrometers AMS [70], BESS [71], and CAPRICE [72]; from the calorimeters ATIC [73] and CREAM [74,75]; from the transition radiation detectors CRN [76] and TRACER [77–79]; from the Čerenkov detector hodoscope HEAO-3 [80]; as well as from the emulsion chamber experiments JACEE [81] and RUNJOB [82].

To extend the measurements of energy spectra up to the knee ($> 10^{15}$ eV) the Advanced Cosmic Ray Composition Experiment for the Space Station (ACCESS) has been proposed [83]. NASA initiated a balloon program in

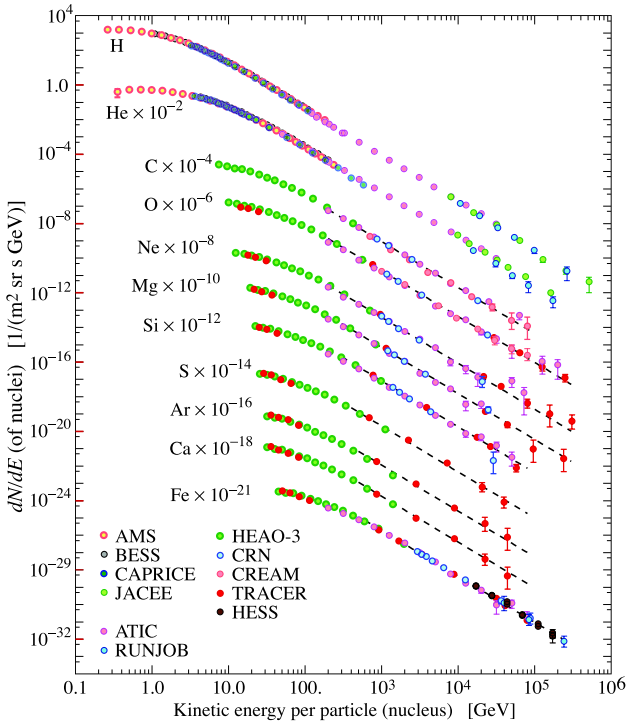

Figure 5. Energy spectra of main elements in cosmic rays [68] and [69] (pg. 254).

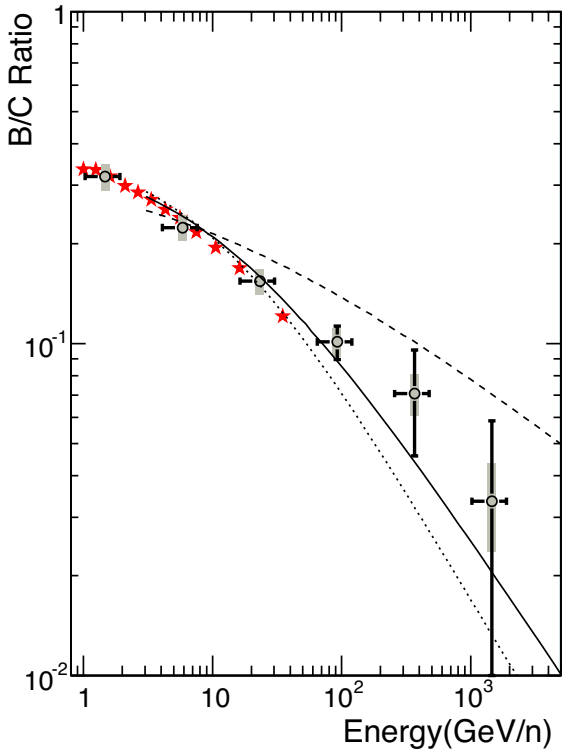

Figure 6. Boron-to-carbon ratio in cosmic rays as measured by the CREAM balloon experiment (circles) and the HEAO-3-C2 space experiment (asterisks) [87]. The thin lines represent statistical uncertainties, the grey bands indicate systematic uncertainties.

support for ACCESS: the transition radiation detector TRACER, the calorimeter ATIC, and CREAM, combining both techniques. Unfortunately, NASA did not select ACCESS for flight neither on the ISS nor as a free-flyer, leaving the balloon payloads as the source of new results. All three experiments are part of the Long Duration Balloon program of NASA [84], providing circumpolar flights from McMurdo, Antarctica. The present record holder in floating time is the CREAM experiment with balloon flights in the seasons 2004/5, 2005/6, and 2007/8 with flight durations of 42, 28, and 29 days, respectively. As can be inferred from Fig. 5 the three experiments deliver results at the highest energies.

The abundances of elements heavier than iron are measured with TIGER [85].

PAMELA, a new space based experiment has been launched in June 2006 and first data have been published [86]. Main components are a magnet spectrometer, a time-of-flight system, an electromagnetic calorimeter, and a neutron detector. PAMELA is expected to yield precise information on electrons, positrons, cosmic-ray nuclei, and anti-nuclei up to energies of several 100 GeV.

To distinguish between different propagation models of cosmic rays in the Galaxy it is of interest to measure the ratio of secondary to primary cosmic rays, e.g. the boron-to-carbon ratio[4]. Measurements indicate that propagation in the Galaxy is energy dependent with the mean path length λ traversed decreasing with increasing energy $\lambda = \lambda_0(R/R_0)^\delta$, with the rigidity $R = E/z$, where E is the energy and z the charge of the particle. Current data, up to about 100 GeV/n, indicate a fall-off in energy with an exponent of

[4] Attention should be payed to not confuse *secondary cosmic rays*, produced during the propagation process in the Galaxy, with *secondary particles*, produced in air showers inside the atmosphere.

$\delta \approx -0.5$ to -0.6. Theories suggest that at high energy the exponent should approach $-1/3$ for a Kolmogorov turbulence spectrum. It is therefore of great interest to extend such measurements to energies as high as possible.

Recent results obtained by the CREAM experiment are depicted in Fig. 6, they extend measurements of the B/C ratio up to 10^3 GeV/n [87]. The lines represent model calculations with values for $\delta = -0.33$ (dashed line), -0.6 (solid line), and -0.7 (dotted line). At high energies the data are compatible with $\delta \approx -0.6$ to -0.5. It is of interest to point out that the grey bars indicate the systematic uncertainties of the measurements. The dominant source of systematic uncertainties at high energy are uncertainties in the cross sections for producing secondaries by charge-changing interactions in the atmosphere above the instrument. Because there is a significant decrease in the interstellar path length with energy, the amount of boron, for example, at high energy is small — making the impact of uncertainties in the atmospheric boron contribution significant above ≈ 100 GeV/n. At these energies the contribution from charge-changing interactions in the atmosphere is similar in size to the total production of boron during propagation through the Galaxy. This emphasizes the importance to measure such cross sections with high precision at accelerators.

One of the hottest topics recently discussed is the discovery of anomalies in the fluxes of electrons and positrons. The ATIC collaboration finds an excess of electrons at energies of $300 - 800$ GeV [88]. The PAMELA group measured an excess in the positron-to-electron fraction $e^+/(e^- + e^+)$ at energies between 10 and 100 GeV [89]. A high precision measurement of the electron spectrum in the energy range from 20 GeV to 1 TeV has been obtained with the Large Area Telescope (LAT) on board the Fermi satellite [90]. The recent data stimulated numerous attempts for a theoretical interpretation of the observed structures (a few hundreds of articles on arXiv). Common explanations include modifications of the diffuse background model due to local sources, contributions of local astrophysical sources such as pulsars, reacceleration at supernova remnants, or dark matter annihilation.

6. TeV Gamma-Ray Astronomy

Many new results from the TeV gamma-ray telescopes H.E.S.S. [91] and MAGIC [92] have been presented. Here we will focus on results which are in particular related to cosmic-ray physics. The measurements of TeV gamma ray emission from supernova remnants strongly supports the theory of Fermi acceleration of hadronic cosmic rays in these objects, see e.g. [93,94]. They provide evidence that (at least a large fraction of) galactic cosmic rays are accelerated in the vicinity of supernova remnants.

The H.E.S.S. Čerenkov telescope system derived for the first time an energy spectrum measuring direct Čerenkov light [95]. This light is emitted by the primary nucleus in the atmosphere before its first interaction, i.e. before the air shower begins [96]. The energy spectrum of iron nuclei has been reconstructed in the energy range between 10 and 100 TeV. The new method is very valuable to bridge the gap between direct measurements and classical air shower measurements, using particle detector arrays.

Also for the first time the primary cosmic-ray electron spectrum has been measured with a ground based detector, the H.E.S.S. experiment [97,98]. An effective gamma-hadron separation algorithm is applied to infer the electron spectrum between 0.3 TeV and about 10 TeV. The result is depicted in Fig. 7. The H.E.S.S. data are compared to measurements with instruments above the atmosphere. A depression of the flux at energies exceeding 1 TeV can be inferred. It is interesting to note that the H.E.S.S. data are compatible with the Fermi measurements at energies around 0.5 TeV, see also last paragraph of Sect. 5.

7. Neutrino Astronomy

In addition to information from charged particles and gamma rays, neutrino astronomy is expected to yield complementary information to reveal the origin of ultra high-energy cosmic rays.

The IceCube neutrino telescope [99,100] is

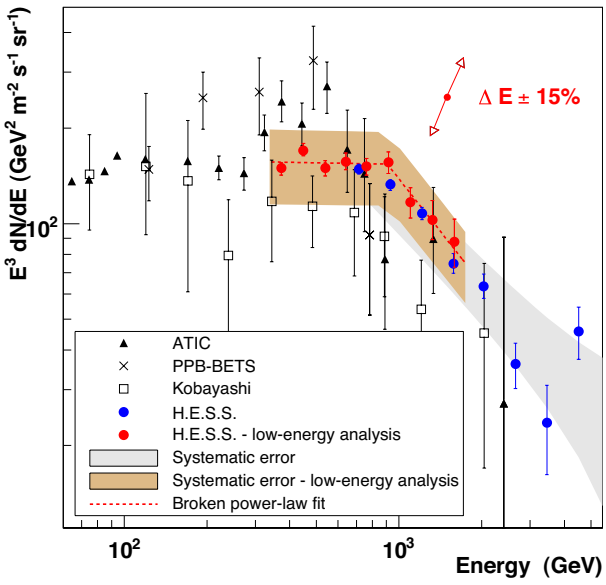

Figure 7. Energy spectrum of primary cosmic-ray electrons $E^3 dN/dE$ as observed by several experiments [97].

presently under construction at the geographical South Pole. It is the successor of the AMANDA experiment, operated till 2009. It is a km^3 detector, comprising 80 strings of 4800 optical modules in total and 80×2 surface detectors (IceTop) [101]. At the time of the conference 80 surface detectors and 40 strings have been deployed. The surface detectors are ice Čerenkov detectors, each equipped with two optical modules.

Data taking and analysis has started with the parts of the experiment already installed. As an example of recent results, the all-sky muon flux as measured with 22 strings is presented in Fig. 8 [99]. Using a combination of minimum bias and muon-filtered data, the performance of IceCube has been verified by comparing the measured muon track zenith angle distribution to a Monte Carlo simulation. For the first time the muon flux was measured over the entire sky using a uniform set of quality parameters. Data and simulation generally agree to better than 20%.

Complementary to the South Pole, neutrino telescopes are under construction in the Mediterranean Sea. The installation of ANTARES [102] has just been completed. It comprises 12 strings,

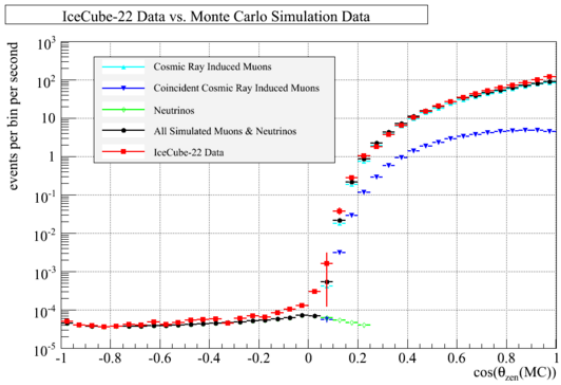

Figure 8. All-sky muon flux as measured with IceCube (22 strings) [99].

each equipped with 75 photo multipliers arranged in 25 "storeys". Data taking has started and first analyses are under way.

The activities of the neutrino telescopes ANTARES, NEMO, and NESTOR are bundled in the KM3NET [103] consortium to build a km^3 neutrino detector in the Mediterranean Sea. At present, various design studies are conducted, construction of the detector is expected to start in 2011 [104].

The Pierre Auger Observatory serves also as detector for high-energy neutrinos [105,106]. The analysis of horizontal air showers yields limits on the neutrino flux in the energy range around 10^{17} to 10^{19} eV which already at present severely constrain exotic models for the origin of ultra high-energy cosmic rays. The upper limits are only about one order of magnitude above the flux expected from neutrinos produced during the propagation of cosmic rays (cosmogenic neutrinos, GZK neutrinos).

8. High-Energy Interactions in the Atmosphere

Air shower data can be used to deduce properties of high-energy hadronic interactions in the atmosphere. This is of particular interest in energy regimes and kinematical regions beyond the capabilities of present-day accelerators.

Frequently, high-energy muons are used to study details of the shower development [107,108].

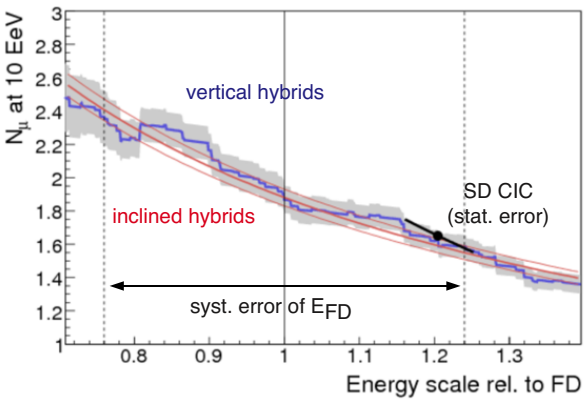

Figure 9. Comparison of the results on the number of muons N_μ at 10 EeV from different methods [115]. Results for vertical and inclined hybrid events are shown as well as results applying the constant intensity method.

Measurement of their production height through triangulation with a tracking detector [109] allows insight into properties of individual hadronic interactions [110]. The OPERA experiment has obtained a new measurement of the muon charge ratio [58].

The KASCADE experiment, measuring simultaneously the hadronic, the electromagnetic, and the muonic shower components is in particular sensitive to details of hadronic interaction models. The data are used to check the consistency of the predictions of hadronic interaction models used in air shower simulations with measured data [111–114]. It could be shown that the recent model EPOS, version 1.6 is not compatible with air shower data. This stimulated the development of a new version 1.9, which is presently under investigation.

The muon content at ground level in the data from the Pierre Auger Observatory has been analyzed in detail at energies around 10 EeV [115,116]. Different sets of hybrid events were used, i.e. the showers have been observed simultaneously with the fluorescence telescopes and the surface detectors. And a constant intensity cut method has been applied to data from the surface detectors. The number of muons is shown as function of the energy relative to the energy scale

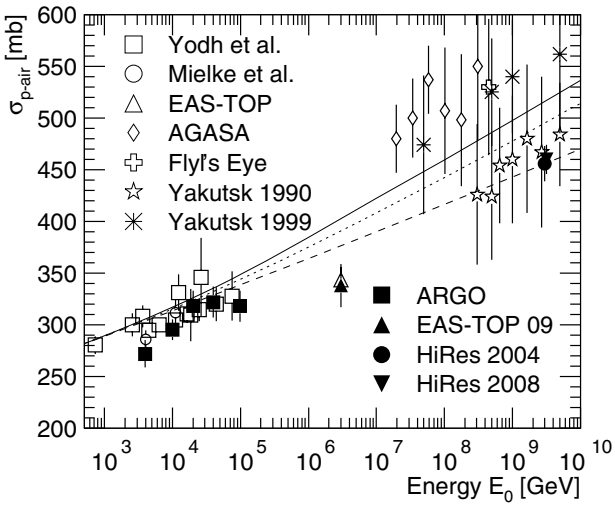

Figure 10. Inelastic proton-air cross section as function of primary energy. For references of the experimental values see text. The lines represent calculated cross-sections for three different versions of the model QGSJET 01, model 1 (original, —), model 2 (· · ·), and model 3 (- - -), see Ref. [117].

of the fluorescence detector in Fig. 9. The investigations reveal that the hadronic interaction models do not predict enough muons at the highest energies.

8.1. Proton-air cross section

The inelastic proton-air cross section has been determined from air shower data. Three techniques can be distinguished to determine the proton-air cross section: investigating unaccompanied hadrons by Yodh et al. [118,119] and Mielke et al. [120]; the N_e/N_μ technique, carefully selecting proton like events as AGASA [121,122], ARGO [123], EAS-TOP 1999 [124] and 2009 [125,126]; as well as analyzing the tail of the measured X_{max} distributions by Fly's Eye [127,128], HiRes 2004 [129] and 2009 [130], and Yakutsk [131]. The experimental values are compiled in Fig. 10 and compared to predictions of the hadronic interaction model QGSJET 01 and a modification, see Ref. [117]. It is interesting to realize that all recent measurements are at the lower edge of the range of measured values.

A thorough systematic study of the effects of the proton-air cross section on air shower observables has been presented by Ulrich [132]. The dependence of the depth of the shower maximum X_{max}, as well as the number of electrons and muons on the inelastic proton-air cross section has been investigated.

The LHC forward detectors, see Sect. 3 will significantly contribute to a better understanding of the proton-air cross section at high energies in the near future.

8.2. Radio Detection of Air Showers

Presently, a very promising technique to detect air showers is revitalized: the measurement of radio emission from air showers [133]. Two experiments are taking data in the energy range around 10^{17} eV: CODALEMA [134,135] and LOPES [136,137]. They register radio frequencies in the range of several tens of MHz. Results of both experiments show clear evidence for a geomagnetic origin of the measured emission in air showers. Most likely, the radio emission is synchrotron radiation generated by electrons and positrons (most of them with energies slightly lower than the critical energy $E_{crit} \approx 84$ MeV) in the magnetic field of the Earth.

A new digital radio telescope LOFAR [138] is presently under construction in the Netherlands and in Europe. With a very high density of antennas (several hundreds of antennas within 2 km diameter in the core) this instrument will be very valuable to study the radio emission in detail, e.g. through precise measurements of the curvature of the shower front.

Radio emission from air showers is also studied at the Pierre Auger Observatory in Argentina [139]. Prototype studies are conducted with setups evolving from the CODALEMA and LOPES experiments. As an example, the arrival direction of air showers registered with radio antennas is depicted in Fig. 11. The arrival directions are clearly non-isotropic, 20 out of 25 events arrive from the South. The maximum number of events measured in East-West polarization direction is registered at arrival directions with an angle of about 90° to the direction of the Earth magnetic field. Similar investigations in the northern hemisphere with CODALEMA and LOPES reveal the same effect. This provides clear evidence for a geomagnetic origin of the observed emission. Main focus of the future activities is the construction of the Auger Engineering Radio Array (AERA) comprising ≈ 150 antennas on an area of about 20 km^2 to measure air showers in the energy range from about 10^{17} to 10^{19} eV [140].

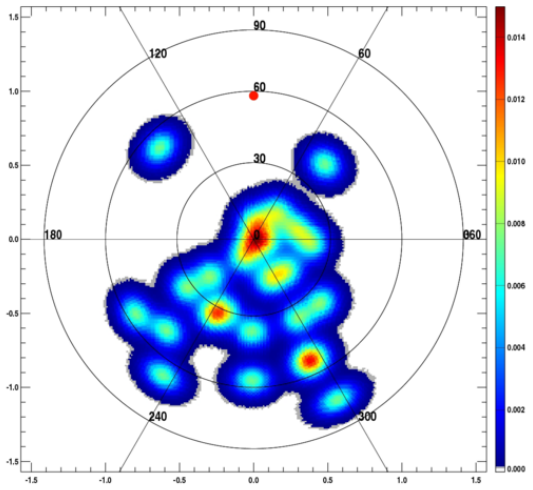

Figure 11. Arrival direction of cosmic rays registered with radio antennas at the Pierre Auger Observatory [134].

9. Indirect Measurements of Cosmic Rays

The anisotropy of cosmic rays in the energy region from 10^{13} to 10^{14} eV has been studied by the Baksan group [142]. An amplitude of a few times 10^{-4} has been observed.

In the energy region of the knee in the spectrum (≈ 10^{15} eV) the Gamma experiment derived an all-particle energy spectrum [143]. The Tibet group reconstructed spectra for primary protons and helium nuclei as well as the all-particle spectrum [144–146]. Spectra for five elemental groups (p, He, CNO, Al, Fe) have been reconstructed with data from the GRAPES experiment [147,148]. KASCADE presented an update on the unfolding of the spectra for groups of elements, different zenith angle intervals have been analyzed and different hadronic interaction

models have been used to interpret the data — the findings confirm earlier results [136,149,150]. The spectra obtained by the different groups fit well into the world data sample and contribute to a consistent picture in the energy region of the knee, see e.g. Ref. [9] and [11] for a comparison of the data. The Tibet group presented ambitious plans to extend their installation. The planned set-up comprises a scintillator array for the electromagnetic component as well as muon detectors: an array of shielded scintillation counters and underground water Čerenkov detectors.

In current astrophysical models a transition from a galactic to an extra-galactic origin of cosmic rays is expected at energies around 10^{17} to 10^{18} eV [11]. A precise measurement of the mass composition in this energy region will be important to distinguish between different astrophysical scenarios.

Several methods are applied to data from the KASCADE-Grande experiment to reconstruct the all-particle spectrum between 10^{16} and 10^{18} eV [136], see Ref. [141] for an update: the constant intensity cut method is applied to measurements of charged particles and muons; the density of charged particles measured at a distance of 500 m to the shower axis S(500) is used; and an unfolding algorithm is applied to electron and muon number data to obtain spectra for groups of elements. The KASCADE-Grande data smoothly continue the all-particle spectrum obtained by KASCADE. Detailed studies of the mass composition are under way.

The 1 km^2 IceTop array [101] at the South Pole is half completed, see also Sect. 7. Data taking has started with the existing parts. First analyses are under way, investigating the lateral distribution of air showers and shower size spectra.

The origin of the highest energy cosmic rays is presently explored with several instruments: the Pierre Auger Observatory is taking data on its southern site [151], also the Telescope Array [152] is fully operational, while the HiRes experiment [153] has stopped data taking. A suppression of the flux has been observed at energies exceeding $4 \cdot 10^{19}$ eV by the HiRes experiment [154] and the Pierre Auger Observatory [155]. One of the most exciting results of the last years is the discovery

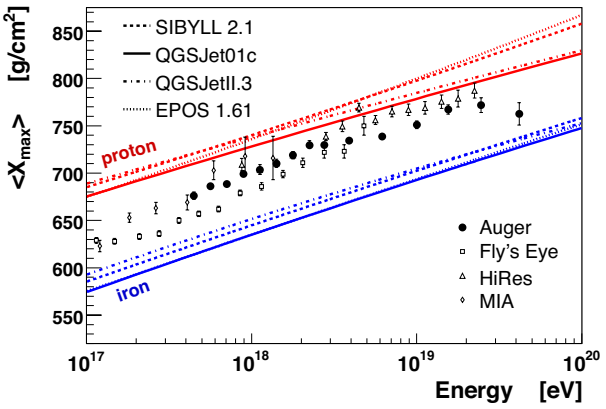

Figure 12. Average depth of the shower maximum X_{max} as function of energy according to different experiments as indicated. The measured values are compared to predictions for primary protons and iron nuclei according to several hadronic interaction models [28].

by the Auger Observatory that the arrival directions of the highest energy cosmic rays are non-isotropic and they are correlated with the position of the supergalactic plane on the sky [156,157].

Different methods are applied to reconstruct the mass composition from Auger data, i.e. the average depth of the shower maximum X_{max} [158], see Ref. [159] for an update: X_{max} is observed directly with the fluorescence telescopes and it is derived from data of the surface detectors investigating the rise time of the signals in the water Čerenkov detectors as well as evaluating the azimuthal asymmetry of the arrival time distributions. Results of the Pierre Auger Observatory are compared to values obtained by other groups in Fig. 12. At the highest energies a trend towards a heavier mass with increasing energy can be recognized.

It is an interesting challenge to combine the latest observations in an astrophysical scenario: the depression in the energy spectrum, the observed anisotropy of the arrival directions, and the development of the mass composition as function of energy. A correlation of the arrival directions with nearby (< 100 Mpc) astronomical objects requires particles with a small charge to have only small deflections in the galactic (and

extra-galactic) magnetic fields. A light composition would also be expected if the observed depression is the GZK effect [160,161]. On the other hand, the data exhibit an increase of the average mass as function of energy. It is also possible that the depression in the spectrum is due to the maximum energy attained during the acceleration process. In this case one would expect a rigidity dependent cut-off behavior of individual elements (similar to the one observed at the knee, but at much higher energies) and one would obtain an increase of the mean mass as function of energy.

At present, the Auger Collaboration is preparing the northern site of the Observatory with an area covering at least 10000 km^2 [162]. This will be an important and mandatory step towards astronomy with charged particles on the full sky.

New experiments are under preparation to observe the fluorescence light of extensive air showers from above the atmosphere. The TUS mission is planned for 2010 with the aim to measure about 10 events/year in the 10^{20} eV energy region [163]. JEM-EUSO is expected to be attached to the Japanese module of the ISS in 2013 to measure cosmic rays with energies exceeding 10^{19} eV [164].

10. Conclusions and Outlook

At the conference a wealth of new data has been presented. They improve our actual knowledge about the origin of high-energy cosmic rays. In the next years many new significant contributions are expected to reveal the origin of high-energy cosmic particles.

The LHC will provide new data on high-energy interactions which will be extremely useful for the interpretation of air shower data.

The atmospheric Čerenkov telescopes H.E.S.S., MAGIC, and VERITAS are taking data and are upgrading their detectors. TeV gamma-ray astronomy has already made significant contributions to the understanding of the sources and the acceleration mechanisms for (charged) cosmic rays. The coming years are expected to lay open more secrets of galactic and extra-galactic sources.

New balloon experiments are under preparation. They will improve our understanding of the propagation of cosmic rays in the Galaxy.

The GRAPES and Tibet groups are currently upgrading their detectors and will provide new data on the composition of cosmic rays in the energy region of the knee in the spectrum ($\approx 10^{15}$ eV).

Several installations are devoted to the energy region of the transition from galactic to extra-galactic cosmic rays ($10^{17}-10^{18}$ eV): KASCADE-Grande, IceCube/IceTop, the low-energy extensions of the Pierre Auger Observatory (HEAT, AMIGA, AERA), as well as the low-energy extension of the Telescope Array (TALE). A precise measurement of the mass composition in this energy region will be crucial to discriminate between different astrophysical scenarios.

The origin of extra-galactic cosmic rays is investigated with set-ups operating at the highest energies: the Telescope Array is fully operational, the southern site of Pierre Auger Observatory is fully operational, the northern site is under preparation, JEM-EUSO is progressing fast.

Also the neutrino telescopes are expected to deliver significant data, ANTARES is fully operational and KM3NET is on good track, IceCube is expected to be completed in 2011.

In summary, we are facing exciting times with big experimental challenges, they will offer unique opportunities and will provide new insights into the (astro)physics of the Universe in the next decade.

11. Acknowledgments

It was a pleasure to summarize the experimental results of this meeting. I would like to thank the organizers for offering such an interesting scientific program. The author is grateful to valuable discussions with his colleagues from the Pierre Auger Observatory, as well as from the KASCADE-Grande, LOPES, LOFAR, and TRACER experiments.

REFERENCES

1. J. Ryan, Proc. 29th Int. Cosmic Ray Conf., Pune 10 (2005) 357.

2. S. Kahler, et al., Proc. 29th Int. Cosmic Ray Conf., Pune 10 (2005) 367.
3. H. Fichtner, Proc. 29th Int. Cosmic Ray Conf., Pune 10 (2005) 377.
4. B. Heber, Int. J. Mod. Phys. A 20 (2005) 6621.
5. T. Gaisser, T. Stanev, Nucl. Phys. A 777 (2006) 98.
6. T. Gaisser, astro-ph/0608553 (2006).
7. A. Strong, et al., Ann. Rev. Nucl. Part. Sci. 57 (2007) 285.
8. J. Hörandel, Astropart. Phys. 19 (2003) 193.
9. J. Hörandel, Adv. Space Res. 41 (2008) 442.
10. J. Hörandel, Nucl. Instr. & Meth. A 588 (2008) 181.
11. J. Blümer, R. Engel, J. Hörandel, Prog. Part. Nucl. Phys. (2009) in press.
12. M. Nagano, A. Watson, Rev. Mod. Phys. 72 (2000) 689.
13. D. Bergman, J. Belz, J. Phys. G: Nucl. Part. Phys. 34 (2007) R359.
14. K.-H. Kampert, arXiv:0801.1986 (2008).
15. J. Hörandel, Rev. Mod. Astron. 20 (2008) 203.
16. R. Engel, Nucl. Phys. B (Proc. Suppl.) 151 (2006) 437.
17. D. Heck, et al., Report FZKA 6019, Forschungszentrum Karlsruhe (1998).
18. H. Fesefeldt, Report PITHA-85/02, RWTH Aachen (1985).
19. A. Fasso, et al., CERN-2005-10, INFN/TC-05/11, SLAC-R-773 (2005).
20. A. Fasso, et al., arXiv:hep-ph/0306267 (2003).
21. J. Ranft, Phys. Rev. D 51 (1995) 64.
22. N. Kalmykov, et al., Nucl. Phys. B (Proc. Suppl.) 52B (1997) 17.
23. S. Ostapchenko, Phys. Rev. D 74 (2006) 014026.
24. S. Ostapchenko, Nucl. Phys. B (Proc. Suppl.) 151 (2006) 143 and 147.
25. R. Engel, et al., Proc. 26th Int. Cosmic Ray Conf., Salt Lake City 1 (1999) 415.
26. K. Werner, F. Liu, T. Pierog, Phys. Rev. C 74 (2006) 044902.
27. T. Pierog, K. Werner, arXiv:astro-ph 0611311 (2006).
28. R. Ulrich, et al., arXiv:0906.3075 (2009).
29. T. McCauley, these proceedings.
30. L. Evans, et al., J. Instr. 3 (2008) S08001.
31. ATLAS Collaboration, J. Instr. 3 (2008) S08003.
32. M. Dova, these proceedings.
33. CMS Collaboration, J. Instr. 3 (2008) S08004.
34. ALICE Collaboration, J. Instr. 3 (2008) S08002.
35. LHCb Collaboration, J. Instr. 3 (2008) S08005.
36. LHCf Collaboration, J. Instr. 3 (2008) S08006.
37. TOTEM Collaboration, J. Instr. 3 (2008) S08007.
38. A. Tricomi, these proceedings.
39. K. Eggert, these proceedings.
40. J. Panman, these proceedings.
41. B. Cole, et al., Proposal 910 submitted to the Fall 1995 BNL HEPNP PAC.
42. I. Chemakin, et al., Phys. Rev. C60 (1999) 024902.
43. I. Chemakin, et al., Phys. Rev. C77 (2008) 015209.
44. M. Catanesi, et al., Nucl. Instr. & Meth. A 571 (2007) 527.
45. R. Raja, Nucl. Instr. & Meth. A (2005) 225.
46. D. Isenhower, et al., arXiv:hep-ex/0609057 (2006).
47. M. Sorel 136 (2008) 022027.
48. S. Afanasiev, et al., Nucl. Instr. & Meth. A 430 (1999) 210.
49. M. Posiadala, arXiv:0901.3332 (2009).
50. M. Adamczyk, et al., Nucl. Instr. & Meth. A 499 (2003) 437.
51. K. Adcox, et al., Nucl. Instr. & Meth. A 499 (2002) 469.
52. B. Back, et al., Nucl. Instr. & Meth. A 499 (2003) 603.
53. K. Ackermann, et al., Nucl. Instr. & Meth. A 499 (2003) 624.
54. T. Lappi, these proceedings.
55. A. Dumitru, et al. 770 (2006) 57.
56. I. Arsene, et al. 93 (2004) 242303.
57. R. Acquafredda, et al., J. Instr. (2009) in press.
58. N. Mauri, these proceedings.
59. Y. Muraki, these proceedings.
60. Y. Muraki, et al., Astropart. Phys. 29 (2008)

229.
61. M. Shea, D. Smart, Proc. 27th Int. Cosmic Ray Conf., Hamburg 8 (2001) 3401.
62. J. Bieber, et al., Astrophys. J. 601 (2004) L103.
63. A. Tylka, et al., Astrophys. J. 625 (2005) 474.
64. E. Vashenyuk, et al., Adv. Space Res. 40 (2007) 331.
65. I. Braun, et al., Adv. Space Res. 43 (2009) 480.
66. C. D'Andrea, J. Poirier, Proc. 28th Int. Cosmic Ray Conf., Tsukuba 6 (2003) 3423.
67. A. Hillas, Ann. Rev. of Astron. and Astroph. 22 (1984) 425.
68. J. Wefel, these proceedings.
69. C. Amsler, et al., Phys. Lett. B 667 (2008) 1.
70. J. Alcaraz, et al., Phys. Lett. B 490 (2000) 27.
71. Y. Ajima, et al., Nucl. Instr. & Meth. A 443 (2000) 71.
72. M. Boezio, et al., Astropart. Phys. 19 (2003) 583.
73. M. Cherry, J. Phys.: Conf. Ser. 47 (2006) 31.
74. P. Maestro, these proceedings.
75. E. Seo, et al., Adv. Space Res. 33 (2004) 1777.
76. D. Müller, et al., Astrophys. J. 374 (1991) 356.
77. F. Gahbauer, et al., Astrophys. J. 607 (2004) 333.
78. D. Müller, et al., Proc. 29th Int. Cosmic Ray Conf., Pune 3 (2005) 89.
79. D. Müller, et al., Proc. 30th Int. Cosmic Ray Conf., Merida 2 (2008) 83.
80. J. Engelmann, et al., Astron. & Astroph. 148 (1985) 12.
81. K. Asakimori, et al., Astrophys. J. 502 (1998) 278.
82. V. Derbina, et al., Astrophys. J. 628 (2005) L41.
83. M. Israel, et al., ACCESS: A Cosmic Journey (Formulation Study Report of the NASA ACCESS Working Group) (2000).
84. W. Jones, Proc. 29th Int. Cosmic Ray Conf., Pune 10 (2005) 173.
85. D. Lawrence, et al., Nucl. Instr. & Meth. A 420 (1999) 402.
86. O. Adriani, these proceedings.
87. H. Ahn, et al., Astropart. Phys. 30 (2008) 133.
88. J. Chang, et al., Nature 456 (2008) 362.
89. O. Adriani, et al., Nature 458 (2009) 607.
90. A. A. Abdo, et al., Phys. Rev. Lett. 102 (2009) 181101.
91. M. Punch, these proceedings.
92. P. Majumdar, these proceedings.
93. H. J. Völk, K. Bernlöhr, Imaging Very High Energy Gamma-Ray Telescopes.
94. E. G. Berezhko, H. J. Völk, arXiv:0812.4198 (2008).
95. F. Aharonian, et al., Phys. Rev. D75 (2007) 042004.
96. D. Kieda, et al., Astropart. Phys. 15 (2001) 287.
97. F. Aharonian, et al., arXiv:0905.0105 (2009).
98. F. Aharonian, et al., Phys. Rev. Lett. 101 (2008) 261104.
99. P. Berghaus, these proceedings.
100. T. DeYoung, arXiv:0906.4530 (2009).
101. T. Stanev, these proceedings.
102. A. Kouchner, these proceedings.
103. D. Dornic, these proceedings.
104. P. Bagley, et al., http://www.km3net.org/CDR/CDR-KM3NeT.pdf.
105. D. Gora, these proceedings.
106. J. Abraham, et al., Phys. Rev. Lett. 100 (2008) 211101.
107. R. Kokoulin, these proceedings.
108. A. Petrukhin, these proceedings.
109. P. Doll, these proceedings.
110. J. Zabierowski, these proceedings.
111. T. Antoni, et al., J. Phys. G: Nucl. Part. Phys. 25 (1999) 2161.
112. W. Apel, et al., J. Phys. G: Nucl. Part. Phys. 34 (2007) 2581.
113. W. Apel, et al., J. Phys. G: Nucl. Part. Phys. 36 (2009) 035201.
114. J. Hörandel, these proceedings.
115. F. Schmidt, et al., arXiv:0902.4613 (2009).
116. F. Schmidt, these proceedings.
117. J. Hörandel, J. Phys. G: Nucl. Part. Phys. 29 (2003) 2439.
118. G. Yodh, et al., Phys. Rev. Lett. 28 (1972) 1005.
119. G. Yodh, et al., Phys. Rev. D 27 (1983) 1183.
120. H. Mielke, et al., J. Phys. G: Nucl. Part. Phys. 20 (1994) 637.
121. T. Hara, et al., Phys. Rev. Lett. 50 (1983)

2058.
122. M. Honda, et al., Phys. Rev. Lett. 70 (1993) 525.
123. G. Aielli, et al., arXiv:0904.4198 (2009).
124. M. Aglietta, et al., Nucl. Phys. B (Proc. Suppl.) 75A (1999) 222.
125. M. Aglietta, et al., Phys. Rev. D 79 (2009) 032004.
126. G. Trinchero, these proceedings.
127. R. Baltrusaitis, et al., Phys. Rev. Lett. 52 (1984) 1380.
128. R. Baltrusaitis, et al., Phys. Rev. D 31 (1985) 2192.
129. K. Belov, et al., Nucl. Phys. B (Proc. Suppl.) 151 (2006) 197.
130. K. Belov, et al., Proc. 30th Int. Cosmic Ray Conf., Merida 4 (2009) 687.
131. M. Dyakonov, et al., Proc. 21st Int. Cosmic Ray Conf., Adelaide 9 (1990) 252.
132. R. Ulrich, these proceedings.
133. H. Falcke, et al., arXiv:0804.0548 (2008).
134. A. Belletoile, these proceedings.
135. D. Ardouin, et al., Astropart. Phys. 31 (2009) 192.
136. A. Haungs, these proceedings.
137. H. Falcke, et al., Nature 435 (2005) 313.
138. J. Hörandel, these proceedings.
139. A. van den Berg, et al., Proc. 30th Int. Cosmic Ray Conf., Merida 5 (2008) 885.
140. A. van den Berg, Proc. 31th Int. Cosmic Ray Conf., Lodz (2009) in press.
141. W. Apel, et al., arXiv:0906.4007 (2009).
142. V. Alexeenko, these proceedings.
143. R. Martisov, these proceedings.
144. J. Huang, these proceedings.
145. M. Amenomori, et al., Astrophys. J. 678 (2008) 1165.
146. M. Amenomori, et al., Phys. Lett. B632 (2006) 58.
147. S. Gupta, these proceedings.
148. Y. Hayashi, et al., Proc. 29th Int. Cosmic Ray Conf., Pune 10 (2005) 243.
149. T. Antoni, et al., Astropart. Phys. 24 (2005) 1.
150. W. D. Apel, et al., Astropart. Phys. 31 (2009) 86.
151. R. Engel, these proceedings.
152. Y. Tameda, these proceedings.
153. P. Sokolsky, these proceedings.
154. R. Abbasi, et al., Phys. Rev. Lett. 100 (2008) 101101.
155. J. Abraham, et al., Phys. Rev. Lett. 101 (2008) 061101.
156. J. Abraham, et al., Science 318 (2007) 938.
157. J. Abraham, et al., Astropart. Phys. 29 (2008) 188.
158. H. Wahlberg, these proceedings.
159. J. Abraham, et al., arXiv:0906.2319 (2009).
160. K. Greisen, Phys. Rev. Lett. 16 (1966) 748.
161. F. Aharonian, J. Cronin, Phys. Rev. D 50 (1994) 1892.
162. D. Nitz, et al., arXiv:0706.3940 (2007).
163. L. Tkatchev, these proceedings.
164. N. Inoue, these proceedings.